Adaptive Hysteresis Band Control for Constant Switching Frequency in Direct Torque Control of Induction Machine Drives

Mustafa AKTAŞ
e-mail: maktas@ktu.edu.tr

H. İbrahim OKUMUŞ
e-mail: okumus@ktu.edu.tr

Karadeniz Technical University, Faculty of Engineering, Department of Electrical & Electronics Engineering, 61100 Trabzon, Turkey

Keywords: Induction Motor, Direct Torque Control, Adaptive Hysteresis Band, and Constant Switching Frequency

ABSTRACT

Hysteresis band control is one of the simplest and most popular techniques used in direct torque control (DTC) of induction machine drives. However the conventional fixed band hysteresis control has a variable switching frequency which causes serious problems in DTC. In this paper, the adaptive hysteresis band control strategy is proposed, where the hysteresis band is controlled in real time as variation of applied voltage vectors. Thereby reducing the torque ripple whilst maintaining a constant torque switching frequency. The proposed adaptive hysteresis band control technique is verified by simulations.

1. INTRODUCTION

Recent advances in power semiconductor and microprocessor technology have made possible the application of advanced control techniques to ac motor drive systems [1]. DTC has become a popular technique for the control of induction motor drives as it provides a fast dynamic torque response and robustness to machine parameter variations without the use of current regulators. The technique can be implemented easily using two hysteresis controllers (one for flux and another for torque) and a switching table to select the switching voltage vector. However, conventional DTC suffers from such effects as torque ripple, variable switching frequency and flux drooping at low speed. These effects result in increased sub-harmonic currents, higher load current ripple and variable switching losses in the inverter [2,3].

This paper proposes a adaptive hysteresis band control strategy, where the hysteresis band is controlled in real time as variation of applied voltage vectors. Thereby reducing the torque ripple whilst maintaining a constant torque switching frequency.

2. GENERAL DESCRIPTION OF DTC

In general, in a symmetrical three-phase induction machine, instantaneous electromagnetic torque is a cross product of the stator and rotor flux linkage space vector or stator current space vector and stator flux linkage space vector.

$$T_e = \frac{3}{2} P \overline{\Psi}_s \times \overline{I}_s \qquad (1)$$

where $\overline{\Psi}_s$ is the stator flux linkage space vector and $\overline{I}_s$ is the stator space vector. In Equation (1), both space vectors are expressed in the stationary reference frame. By considering that $\overline{\Psi}_s = L_s \overline{I}_s + L_m \overline{I}_r^{'}$ $\overline{\Psi}_r' = L_r \overline{I}_r + L_m \overline{I}_s$ where the primed rotor quantities are expressed in the stationary reference frame, it follows that $\overline{I}_s = \overline{\Psi}_s / L_s^{'} - \left[L_m / (L_r L_s^{'}) \right] \overline{\Psi}_r^{'}$. Thus equation (1) takes the following from

$$T_e = \frac{3}{2} P \frac{L_m}{L_s^{'} L_r} \left| \overline{\Psi}_r^{'} \right| \left| \overline{\Psi}_s \right| \sin \gamma \qquad (2)$$

The electromagnetic torque given by equation (2) is a sinusoidal function of γ, the angle between the stator and rotor flux linkage space vector.

The magnitude of the stator flux is normally kept constant and the motor torque controlled by means of the angle γ. The rotor time constant of the standard induction machine is typically larger than 100 ms, thus the rotor flux is stable and its stable and its variations is slow compared with the stator flux. It is therefore possible to achieve the required torque very effectively by rotating the stator flux vector directly in a given direction as fast as possible.

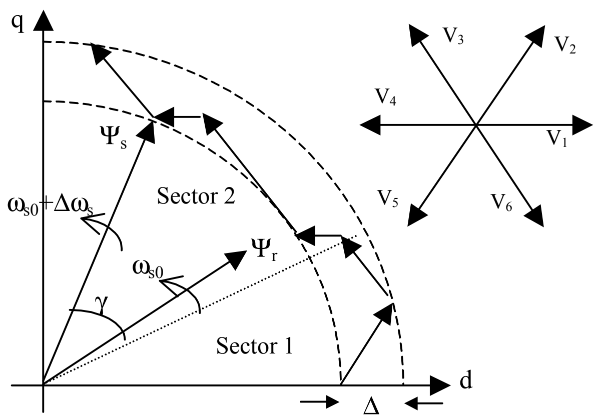

Figure 1. Optimum voltage vector in the torque control and voltage vectors

Figure 1 shows stator flux behaviour compared to rotor flux, after a step variation stator pulsation, $\omega_{s0}=\omega_{s0}+\Delta\omega_s$, with ω_{s0} the initial pulsation and $\Delta\omega_s$ the step variation. Controlling the stator flux stator flux and electromagnetic torque control achieved by using the appropriate stator voltages can quickly change the electromagnetic torque. Choosing suitable voltage vectors those increases or decreases γ causes the electromagnetic torque to increase or to decrease [4].

Table 1. Switching table

dψ	dt$_e$	sector 1	sector 2	sector 3	sector 4	sector 5	sector 6
1	1	V_2	V_3	V_4	V_5	V_6	V_1
	0	V_7	V_0	V_7	V_0	V_7	V_0
	-1	V_6	V_1	V_2	V_3	V_4	V_5
0	1	V_3	V_4	V_5	V_6	V_1	V_2
	0	V_7	V_0	V_7	V_0	V_7	V_0
	-1	V_5	V_6	V_1	V_2	V_3	V_4

The core of the system consists of a flux and torque estimator, a speed controller, a flux controller, a torque controller and an optimum switching table. The estimator estimates the actual stator flux and torque using two measured motor stator phase currents, the dc voltage and the states of the power switches. Torque and flux references are compared with the actual values and a two-level for flux and a three-level for torque hysteresis control method produces control signals.

3. HYSTERESIS BAND CONTROL IN DTC

The hysteresis band control method is a simple and common form of closed-loop control. The block diagrams for the two-level and three-level hysteresis band control methods are shown figures below. Hysteresis band control is widely used because of its abilitiy to be simply implemented. Besides the fast response the inherent peak current limiting capability and excellent dynamic performance that is offers, it does not require an accurate knowledge of the load parameters. In addition, hysteresis band control is essentially an analog technique. Despite the advantages given by the digital controllers, in terms of interfacing, maintenance, flexibility, and integration, their accuracy and response speed are often insufficient for current control in highly demanding applications, such as active filters and high precision drives. In a DTC scheme,

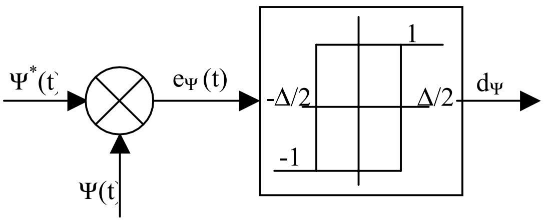

Figure 2. Block diagram of two-level Hysteresis Band Control

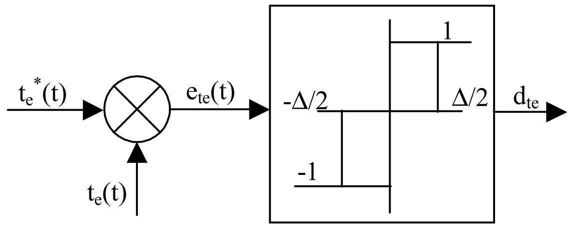

Figure 3. Block diagram of three-level Hysteresis Band Control

the objective is to reduce both the stator flux and torque errors to zero using hysteresis comparators select the optimum voltage vector. Hysteresis comparators lie at the heart of DTC schemes and are responsible not only for determining the optimum voltage vector to be switched, but also for determining how long that vector or action remains selected. Hysteresis is used to prevent the power devices from switching unnecessarily at each new update or switching decision. In this study, a two level hysteresis comparator, as shown Figure 2, used in DTC to compare the actual value of stator flux to the internal reference value produced by stator flux reference controller. In the similar manner, a three level hysteresis comparator, as shown in Figure 3, is used to compare the actual value of the torque to the internal reference value produced by the speed torque reference controller [4]. The outputs of these comparators are update every sampling time and they indicate whether the flux or torque has to be varied.

4. ADAPTİVE HYSTERESİS BAND STRATEGY

In a DTC scheme, for fixed torque band amplitude ΔT_e, the inverter switching frequency is related to the amplitude of the flux hysteresis band $\Delta\Psi$. A small flux hysteresis bandwidth results in a higher switching frequency, the stator flux vector locus approaches a circle and the phase current waveform is nearly sinusoidal. These operating conditions result in low harmonic copper losses in the machine while switching losses in the inverter are high. Alternatively, a large hysteresis bandwidth for stator flux decreases the switching frequency and the stator flux vector locus becomes a hexagon. In this case the switching losses decrease in the inverter while the harmonic copper losses increase in the machine [5].

Adaptive hysteresis band has been well investigated as a two level strategy. The adaptive hysteresis band strategy can be extended to three level hysteresis band. It is demonstrated that adapting the width of the hysteresis band for the three level strategy as a function of pulse number FR and depth M. The block diagram of three level hysteresis band to be analysed is illustrated Figure 4. Output $t_e(t)$ tracks the reference function $t_e^*(t)$ to within a band whose limit is $\Delta+\Sigma$. It is important to note the Σ quantity is required only to create the three voltage level in the output of the hysteresis element. In simulation results Σ is decrease down a very small value and for the simulation results presented in this paper it was set to be Δ/100.

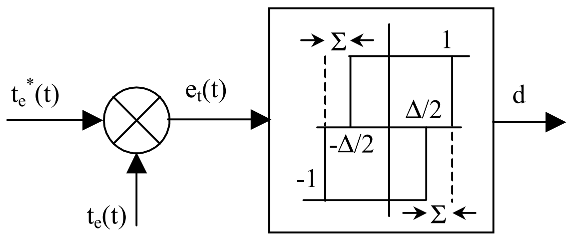

Figure 4 Block diagram of three level adaptive hysteresis band control

Adaptive hysteresis band is herently an analogue process because switching is produced at the intersection of the error between $t_e^*(t)$ and $t_e(t)$ and the adaptive hysteresis band limits. The equations describing these intersection points are nonlinear and transcendental and

$$p = \frac{\left[\left(t_e(t_2) + \frac{\Delta}{2}\right) - \left(t_e(t_1) - \frac{\Delta}{2}\right)\right]}{t_2 - t_1} \qquad (3)$$

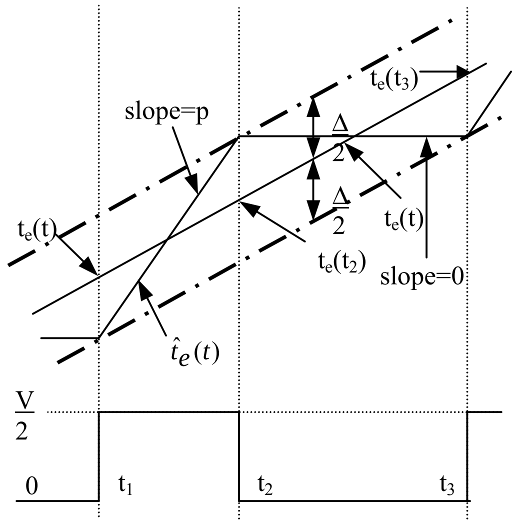

Figure 5. Production of one pulse for three level adaptive hysteresis band control

therefore must be solved off-line. The following analysis illustrates the pulse-position that occurs in three-level adaptive hysteresis band control. The production of one pulse for the three-level adaptive hysteresis band control method is illustrated in Figure 5 to explain the analysis in below. By inspection of Figure 5 the slope of the signal $t_e(t)$ when the output is +V/2 can be described as. It is necessary to assume a fixed slope for the reference function to describe the adaptive hysteresis band process as a continuous function of time. This assumption has not been found to produce significant errors in the switching angles using the analogue simulation [5]. By assuming a fixed gradient of $t_e(t)$ over each switching period the "on" or t_2-t_1 time can be approximated as

$$t_{on} = \frac{\Delta}{p - t_e'(t)} \qquad (4)$$

The slope of output signal $\hat{t}_e(t)$ during the time $t_2<t<t_3$ is zero because the output voltage is zero in this time period. Therefore from inspection of Figure 5, the slope of the reference function can be expressed as

$$t_e'(t) \approx \frac{t_e(t_3) - t_e(t_2)}{t_3 - t_2} = \frac{\Delta}{t_3 - t_2} \qquad (5)$$

and therefore the corresponding off time may be expressed as

$$t_{off} = t_3 - t_2 = \frac{\Delta}{t_e'(t)} \qquad (6)$$

By combining equation (4) and (6) the total instantaneous time period T_i is described as

$$T_i = t_{on} + t_{off} = \frac{\Delta}{p - t_e'(t)} + \frac{\Delta}{t_e'(t)} \qquad (7)$$

The corresponding instantaneous angular frequency, ω_i, is determined by equation (8)

$$\omega_i = \frac{2\pi}{T_i} \qquad (8)$$

The carrier frequency, ω_c, which determines the pulse number is the average value of the instantaneous frequency, ω_i, over one fundamental period and is expressed as

$$\omega_c = \frac{2}{\Delta p}\left[2A\omega p - \frac{A^2\omega^2\pi}{2}\right] \qquad (9)$$

The analysis presented has demonstrated that the pulse number, FR, is a function of reference function amplitude, A, slope, p, of the output signal, $\hat{t}_e(t)$, and the width of the hysteresis band, Δ. Therefore, it is necessary to adapt the width of the hysteresis band so that it has a constant width along a fundamental period according to Equation (10). This enable only the pulse number, FR, and depth, M, to be the specified parameters in the modulation process [5]. Therefore, the width of the adaptive hysteresis band can be expressed as

$$\Delta = \frac{4Mp}{\omega_c}\left[1 - \frac{M\pi}{4}\right] \qquad (10)$$

where $\omega_c = FR\omega$, and the depth, M, is defined as

$$M = \frac{A\omega}{p} \qquad (11)$$

5. SIMULATION RESULTS

A simulation study for the proposed adaptive hysteresis band control technique was carried out using the matlab software package. The motor parameters used in the simulations are given in the appendix.

In the simulation the proposed DTC drive is operated in the speed control mode with a load of 10 nm and stator flux and rotor speed references of 0.8wb and 200 rad/s respectively. When fig. 7(b) are fig. 8(b) are compared it is observed that fig. 8(b) is circular while fig. 7(b) looks like a hexagon. It should be noted that the effect of the proposed scheme can be seen very easily at low speed from the simulation results. Constant inverter switching frequency is obtained by using adaptive hysteresis bandwidth. Furthermore, inverter switching frequency with adaptive hysteresis band is obtained and this is illustrated in figure 6. in addition, switching frequency is small at low speeds. In order to increase the switching frequency the torque adaptive hysteresis band width is decreased. Thus stator flux locus becomes circular. In conclusion, the obtained simulation results fig. 7(a) and 8(a), fig. 7(b) and 8(b), fig. 7(c) and 8(c), fig. 7(d) and 8(d) are shown for comparison.

6. CONCLUSIONS

In this paper a adaptive hysteresis band control strategy, where the band is controlled as variation of applied voltage vectors in order to keep the switching frequency constant at any operating conditions is proposed. The proposed control technique is verified by simulations. With proposed technique, the switching frequency of the inverter is nearly held constant.

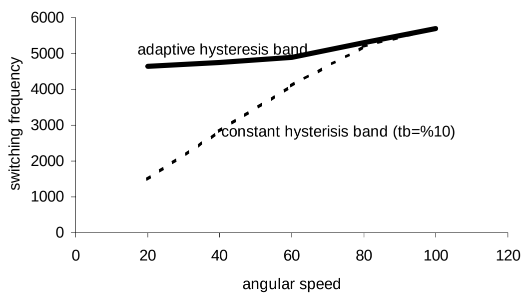

Figure 6. Effect to switching frequency of adaptive hysteresis band control.

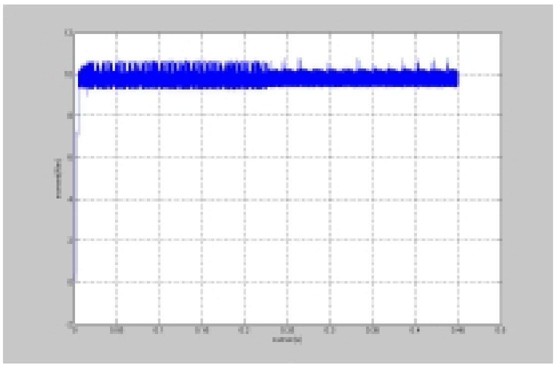

a) Electromagnetic torque, T_e (or t_e)

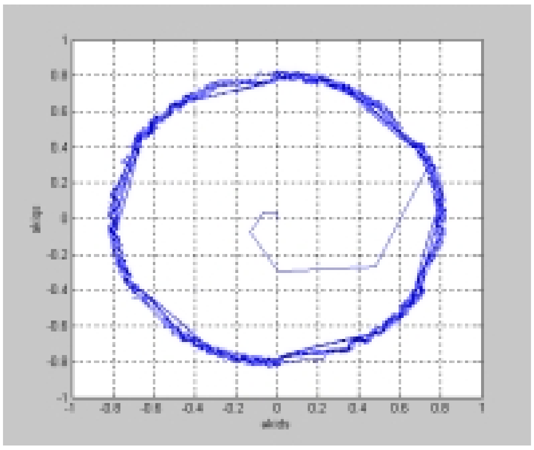

b) Stator flux vector locus (Ψ_{ds}-Ψ_{qs})

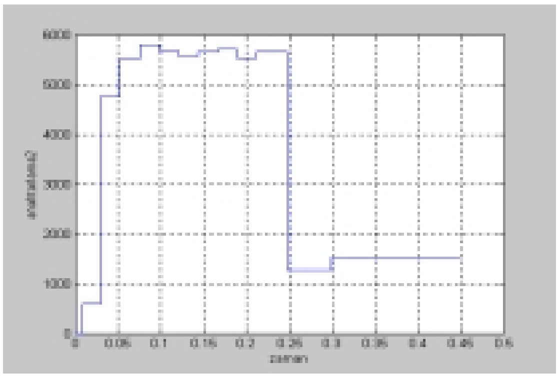

c) Switching frequency, f_c

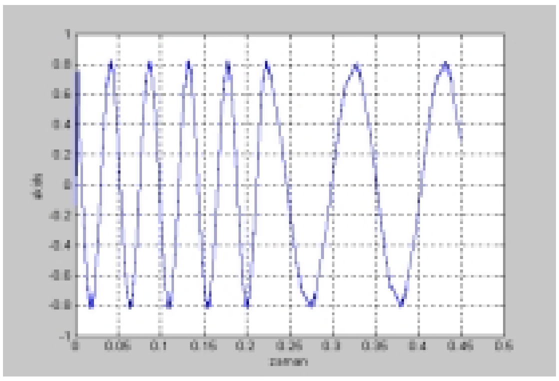

d) Stator flux vector Ψ_{ds}

Figure 7. Fixed hysteresis band (t_{band}=%10)

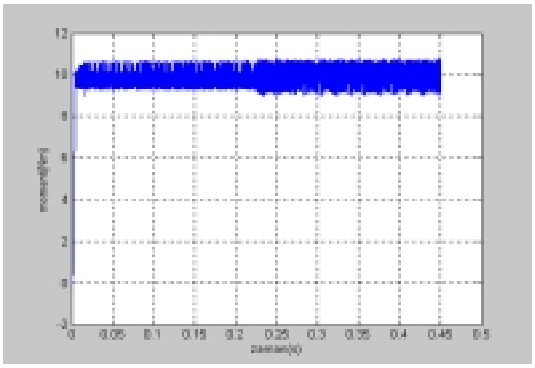

a) Electromagnetic torque T_e (or t_e)

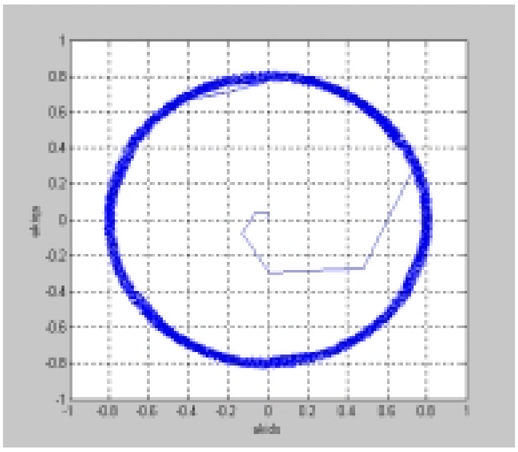

b) Stator flux vector locus (Ψ_{ds}-Ψ_{qs})

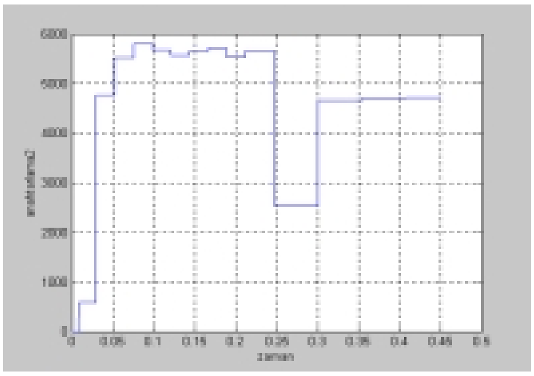

c) Switching frequency f_c

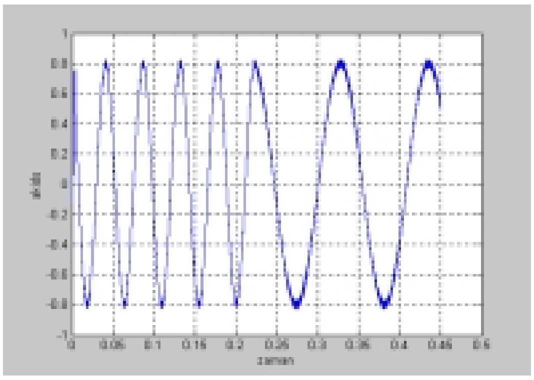

d) Stator flux vector Ψ_{ds}

Figure 8. Adaptive hysteresis band

REFERENCES

1. Bose Bimal K., An Adaptive Hysteresis-Band Current Control Technique of a Voltage-Fed PWM Inverter for Machine Drive System, IEEE TRANS. IND. ELECTRON., vol 37, pp. 402-408, Oct. 1990
2. Casadei D, Grandi G, Serra G, Effects of Flux and Torque Hysteresis Band Amplitude in Direct Torque Control of Induction Machines, IECON'94, Bologna, Italy, 5-9 September 1994, pp.299-304.
3. J.K.Kang, D.W. Chung, S.K. Sul, Direct Torque Control of Induction Machine With Variable Amplitude Control of Flux and Torque Hysteresis Bands, IEEE/ IEMD Intn. Conf. (1999) 640-642.
4. Okumuş H. İ., Improved Direct Torque Control of Induction Machine Drives Phd Thesis, UNİVERSİTY OF BRİSTOL, UK, July 2001
5. Bowes S.R, Grewal S, Three-level hysteresis band modulation strategy for single-phase PWM inverter, IEEE Proc.-Electr. Power Appl., Vol. 146, No 6, November 1999
6. I. Takahashi, T. Noguchi, A New Quick-Response and High-Efficiency Control Strategy of an Induction Motor, IEEE Trans. Industry App. IA-22 (1986) 820-827.
7. P. Vas, Sensorless vector and direct torque control, Oxford University Press, New York, 1998.
8. J.K. Kang, S.K. Sul, New Direct Torque of Induction Motor for Minimum Torque Ripple and Constant Switching Frequency, IEEE Trans. Industry App., 35 (1999) 1076-1082.

Appendix

Motor Parameters Used For the Simulation

R_s = 3 Ω, R_r = 5.6 Ω, L_s = L_r =0.1 H, M = 0.09 H